ELSEVIER

Chemical Geology 220 (2005) 315–327

CHEMICAL GEOLOGY
INCLUDING
ISOTOPE GEOSCIENCE

www.elsevier.com/locate/chemgeo

Competition between enzymatic and abiotic reduction of uranium(VI) under iron reducing conditions

Thilo Behrends*, Philippe Van Cappellen

Utrecht University, Department of Earth Sciences-Geochemistry, P.O. Box 80021, NL-3508 TA, Utrecht, The Netherlands

Received 25 May 2004; received in revised form 30 March 2005; accepted 14 April 2005

Abstract

Reduction of U(VI) under iron reducing conditions was studied in a model system containing the dissimilatory metal-reducing bacterium *Shewanella putrefaciens* and colloidal hematite. We focused on the competition between direct enzymatic uranium reduction and abiotic reduction of U(VI) by Fe(II), catalyzed by the hematite surface, at relatively low U(VI) concentrations (<0.5 μM) compared to the concentrations of ferric iron (>10 mM). Under these conditions surface catalyzed reduction by Fe(II), which was produced by dissimilatory iron reduction, was the dominant pathway for uranium reduction. Reduction kinetics of U(VI) were identical to those in abiotic controls to which soluble Fe(II) was added. Strong adsorption of U(VI) at the hematite surface apparently favored the abiotic pathway by reducing the availability of U(VI) to the bacteria. In control experiments, lacking either hematite or bacteria, the addition of 45 mM dissolved bicarbonate markedly slowed down U(VI) reduction. The inhibition of enzymatic U(VI) reduction and abiotic, surface catalyzed U(VI) reduction by the bicarbonate amendments is consistent with the formation of aqueous uranyl-carbonate complexes. Surprisingly, however, more U(VI) was reduced when dissolved bicarbonate was added to experimental systems containing both bacteria and hematite. The enhanced U(VI) reduction was attributed to the formation of magnetite, which was observed in experiments. Biogenic magnetite produced as a result of dissimilatory iron reduction may be an important agent of uranium immobilization in natural environments.

Keywords: Enzymatic U(VI) reduction; Surface catalyzed U(VI) reduction; Iron respiration; Biogenic magnetite; Hematite; *Shewanella putrefaciens*

1. Introduction

The reduction of uranyl to the tetravalent state has a marked effect on the mobility of uranium in the environment. Under natural conditions uraninite (UO_2(c)), pitchblende (UO_2(am)) and coffinite ($USiO_4$), the most common salts of the uranous ion U^{4+}, have much lower solubilities than salts of the uranyl ion (UO_2^{2+}) (Langmuir, 1997). Additionally, the uranyl ion forms strong aqueous complexes with carbonate (Grenthe et al., 1992; Langmuir, 1997), inhibiting precipitation or sorption of U(VI) in alka-

* Corresponding author. Fax: +31 30 253 5302.
E-mail address: behrends@geo.uu.nl (T. Behrends).

0009-2541/$ - see front matter © 2005 Elsevier B.V. All rights reserved.
doi:10.1016/j.chemgeo.2005.04.007

line waters. Consequently, uranium reduction is a key process in risk assessment of nuclear waste repositories, the remediation of sites contaminated with uranium, the formation of uranium ore deposits, and the global cycling of this element.

Reduction of U(VI) generally coincides with microbial iron and sulfate reduction. A variety of sulfate and metal-reducing bacteria are capable of reducing U(VI) (Caccavo et al., 1992; Francis et al., 1994; Lovley and Phillips, 1992; Lovley et al., 1991; Tebo and Obraztsova, 1998; Wade and DiChristina, 2000). Incubation experiments in which U(VI) was added to groundwaters and soils taken from uncontaminated sites and sites contaminated with uranium have revealed the ubiquitous presence of uranium-reducing microbial communities (Abdelouas et al., 2000). Nonetheless, the microbial reduction mechanisms in suboxic and anoxic environments remain poorly known.

The reduction of U(VI) by the products of iron and sulfate respiration, ferrous iron (Fe(II)) and sulfide, is thermodynamically possible, while methane and hydrogen are also potential reductants (Langmuir, 1978). The abiotic reduction of U(VI) by dissolved sulfide in homogeneous solution has been demonstrated (Ho and Miller, 1986; Kosztolanyi et al., 1996; Mohagheghi et al., 1985). The homogenous reaction is favored by high temperature, high sulfide concentrations and high pH-conditions unlikely to occur in sediments and groundwaters. Wersin et al. (1994) investigated the adsorption of uranium onto galena and pyrite using spectroscopic techniques. They observed reduction of U(VI) at the solid–aqueous solution interface and suggested that heterogeneous reduction may be an important process in the genesis of roll-type uranium deposits.

Liger et al. (1999) studied the reduction of U(VI) by ferrous iron. In their experiments, they found no indication of homogeneous reduction of U(VI) by Fe^{2+} ions, but showed that the reaction is catalyzed by iron (hydr)oxides. They explained the dependency of the reduction rate on pH and ferrous iron concentration by postulating that the neutral hydroxo surface complex ($\equiv Fe^{III}OFe^{II}OH^{0}$) is the reactive reductant species. They proposed the following rate law for U(VI) reduction:

$$\frac{d[U(VI)]}{dt} = -k\left[\equiv Fe^{III}OFe^{II}OH^{0}\right][U(VI)]_{ads} \qquad (1)$$

with $k = 399 \pm 25$ M^{-1} min^{-1}, at 25 °C, and $[U(VI)]_{ads}$ is the uranyl concentration adsorbed onto the hematite surface.

Under suboxic conditions, U(VI), rather than Fe(III), is considered the preferred terminal electron acceptor for microbial respiration, due to a higher energetic yield (Cochran et al., 1986; Fredrickson et al., 2000). Wielinga et al. (2000) found that the presence of goethite and hematite did not significantly affect enzymatic reduction of U(VI) coupled to the oxidation of an organic electron donor. The presence of ferrihydrite, however, decreased the initial reduction rate of U(VI). In mixtures of goethite and ferrihydrite, the inhibition was related to the fraction of ferrihydrite. Fredrickson et al. (1998) observed no effect on the reduction of U(VI) to U(IV) when goethite was added and when U(VI) occurred predominantly as the carbonate complexes $UO_2(CO_3)_3^{4-}$ and $UO_2(CO_3)_2^{2-}$, or as the mineral metaschoepite [$UO_3 2H_2O(s)$]. The reduction of uranium was incomplete when U(VI) precipitated as metaschoepite or when lactate, the electron donor, was limiting. They proposed that the precipitation of $UO_2(s)$ or $Fe(OH)_3(s)$ on the metaschoepite surface physically prevented U(VI) from being reduced.

Previous experimental work clearly demonstrates the important role of the chemical speciation of Fe(III) and U(VI) in microbial reduction processes. Much of the previous work, however, was carried out at relatively high U(VI) concentrations. Fredrickson et al. (1998) and Wielinga et al. (2000), for example, performed their experiments at uranium concentrations above 100 μmol/L. While these uranium levels are relevant for contaminated sites, in non-polluted environments uranium concentrations are much lower, and the ratio between U(VI) and Fe(III) is generally much smaller than in the laboratory experiments. High Fe(III) to U(VI) ratios favor adsorption of U(VI) to ferric iron (hydr)oxides. Under these conditions, surface catalyzed reduction by Fe(II) may become the preferred reaction pathway. Rate constants measured by Liger et al. (1999) for the surface catalyzed reduction by Fe(II) indicate that this pathway could outcompete enzymatic U(VI) reduction under typical conditions encountered in suboxic environments.

In this paper, we focus on the competition between alternative pathways of uranium reduction under iron reducing conditions at relatively low U(VI) concen-

trations (<0.5 μM). For this purpose we used a model system containing nanoparticulate hematite, as the Fe(III) substrate, and the facultative anaerobic bacterium *Shewanella putrefaciens*. This organism was selected because it is capable of using a broad variety of electron acceptors, including ferric iron and U(VI), for respiration (Blakeney et al., 2000).

2. Methods

2.1. Bacterial strains

S. putrefaciens strain 200 was originally isolated from crude oil (Obuekwe et al., 1981). A spontaneous rifamycin-resistant strain 200R and a mutant deficient in growth with U(VI) as sole electron acceptor (strain U14) were provided to us by Dr. Thomas DiChristina of Georgia Institute of Technology, Atlanta, Georgia (DiChristina and DeLong, 1994; Wade and DiChristina, 2000).

2.2. Preparation of mineral and cell suspensions

Bacteria were grown aerobically to late log phase at room temperature in Lauria Bertani medium (10 g L^{-1} tryptone, 10 g L^{-1} NaCl, 5 g L^{-1} yeast extract). Bacterial suspensions were centrifuged (2083×*g*, 15 min) and resuspended in 0.1M NaCl solution or in a salt solution with the same composition as the medium of the incubation experiment, but omitting lactate. After repeated washing, the bacterial suspensions were transferred into septa flasks and sealed airtight with butyl stoppers. The suspensions were flushed 30 min with argon prior to use in anaerobic incubations.

Hematite was synthesized as described by Liger et al. (1999): 100 mL of a 0.1 M $Fe(NO_3)_3$ solution were added to 1 L of boiling demineralized water at a rate of 3 mL min^{-1}. After the suspensions cooled down they were transferred into dialysis tubes and placed in demineralized water whose pH was adjusted to pH 4 with 0.1 M HCl. (Note: HCl instead of HNO_3 was used because NO_3^- can be used as an electron acceptor by *S. putrefaciens*.) The water was replaced after equilibration for a minimum of 2 days. The procedure was repeated at least 4 times, until the pH remained unchanged resulting in a dilution factor of over 3000. Hematite was kept in suspension at pH 4 until used in the experiments. It was purged 30 min with Ar prior to use in the anaerobic incubation experiments.

The size of the primary particles, estimated from X-ray diffraction measurements, was 8 ± 2 nm, based on the Williamson–Hall reciprocal space method (D. Rancourt, University of Ottawa, Canada, personal communication). The specific surface area, determined by nitrogen adsorption BET, was 129 m^2 g^{-1}. Particle size and specific surface area indicate that our hematite particles were slightly smaller than those synthesized by Liger and coworkers.

2.3. Experimental methods

2.3.1. Abiotic reduction of U(VI)

The abiotic reduction of U(VI) by Fe(II) was investigated in hematite suspensions in a glove box under Ar atmosphere at 25 °C. Solid $NaNO_3$ was added to 100 mL of a hematite suspension (0.53 g L^{-1}) giving a final concentration of 0.1 mol L^{-1}. The pH was adjusted to 7.5 with 0.01 M NaOH or 0.01 M HCl using an automatic titrator (Metrohm GP736) controlling a burette installed in the glove box. After equilibration, $FeSO_4$ stock solution was added ($[Fe(II)]_t = 1.6 \times 10^{-4}$ M) and, after 30 min equilibration time, the experiment was started by adding uranyl acetate stock solution ($[U(VI)]_0 = 5 \times 10^{-7}$ M). Over the course of an experiment aliquots of the reaction medium were periodically retrieved with a syringe. During the experiment, and during pre-equilibration with Fe(II), the pH was kept constant at 7.5 with a pH-stat and the consumption of base was monitored.

2.3.2. Reduction of U(VI) in the presence of S. putrefaciens

Reduction of U(VI) in the presence of *S. putrefaciens* was studied with the two different strains, 200R and U14. The bacteria+hematite experiments were performed in 50 mL centrifuge tubes at 25 °C in a glove box under Ar atmosphere. Bacteria were added to a hematite suspension containing hematite (0.53 g L^{-1}), lactate (20 mM), KCl (5.6 mM), NH_4Cl (19 mM), Na_2SO_4 (14 mM), $CaCl_2$ (1.3 mM), and $MgSO_4$ (0.43 mM). Before adding the bacteria the pH of the medium was adjusted to 7.5 with 0.1 M NaOH. Bacterial cell densities were approximately 5×10^8 cells mL^{-1}. The tubes were vertically rotated in a

glove box. Aliquots were taken periodically with a syringe for analysis. After 48 h, the Fe(II) concentration reached a value of about 0.5 mM as a result of microbial iron reduction. At that point uranyl acetate stock solution was added ($[U(VI)]_0 = 5 \times 10^{-7}$ M).

Control experiments were performed by omitting either hematite or bacteria. In a number of control experiments, $FeSO_4$ solution ($[Fe(II)]_t = 1.6 \times 10^{-4}$ M) was added. Preliminary experiments were run to test whether the abiotic, surface catalyzed reduction of U(VI) was different in 0.1 M $NaNO_3$ hematite suspensions, compared to hematite suspensions in medium consisting of lactate (20 mM), KCl (5.6 mM), NH_4Cl (19 mM), Na_2SO_4 (14 mM), $CaCl_2$ (1.3 21 mM), and $MgSO_4$ (0.43 mM). No significant effects of the presence of lactate or differences in the background electrolyte were observed.

2.3.3. Effect of bicarbonate on iron and uranium reduction

S. putrefaciens 200R was added to hematite suspensions containing hematite (2.0 g L^{-1}), lactate (20 mM), and either NaCl (45 mM) or $NaHCO_3$ (45 mM). In contrast to the previous experiments, uranyl acetate ($[U(VI)]_0 = 5 \times 10^{-7}$ M) was added together with the bacteria. Bacterial cell densities were about 2.8×10^8 cells mL^{-1}. The pH was adjusted to 7.5 with 0.01 M NaOH or 0.01 M HCl using an automatic titrator (Metrohm GP736). The experiments were performed in 50 mL centrifuge tubes, which were vertically rotated in a glove box under Ar atmosphere. Periodically, an aliquot was collected with a syringe for analysis and the pH of the medium was readjusted. In control experiments either hematite or bacteria were omitted.

2.4. Analytical methods

2.4.1. Cell numbers

Cell numbers were determined according to the method of Hobbie et al. (1977). Bacteria were stained with acridine orange after dilution of the samples to cell densities of about 10^7 cells mL^{-1}; 50 μL of stained cell suspension were diluted with 10 mL filtered acridine orange containing 0.01 M NaCl solution in a filtration funnel. Cells were collected by filtration on an Isopore™ 0.2 μm poresize GTBP membrane filter and counted by epifluorescence microscopy, using the image analysis program analySIS Pro 3.00 (SIS GmbH).

2.4.2. Uranium analysis

Uranyl was selectively extracted by bicarbonate (Liger et al., 1999), by mixing 1 mL of suspension with 4 mL of 0.5 M $NaHCO_3$ in a disposable syringe. After 20 min, the suspension was filtered through a 0.2 μm poresize Acrodisc GHP filter into a 15 mL disposable polypropylene tube. The solution was acidified with 0.4 mL concentrated nitric acid (suprapur) to degas carbon dioxide, and the uranium concentration was determined by inductively coupled plasma mass spectrometry (ICP-MS). Uranium concentrations in the extracts were considered to represent total U(VI). Dissolved U(VI) was quantified by directly filtering 1 mL of suspension through a 0.2 μm poresize Acrodisc GHP filter and omitting the extraction step.

The filtration step was found to efficiently retain the nanoparticulate hematite, because the latter formed aggregates exceeding the poresize of the filters, under the experimental conditions. We also tested whether possible colloidal products of uranium bioreduction (Suzuki et al., 2002) might pass through the filters, using the selective solvent extraction method of Bertrand and Choppin (1982). Suspensions obtained at the end of microbial U(VI) reduction experiments without hematite present were extracted at pH 0.6 with thenoyltrifluoroacetone. Uranium concentrations measured in the extracts confirmed that significant fractions of the initially added U(VI) were transformed into U(IV) due to microbial reduction. However, no detectable U(IV) was found in the filtrates of the suspensions, implying that all reduced uranium was retained on the 0.2 μm poresize Acrodisc GHP filters.

2.4.3. Iron analysis

Total concentrations of ferrous iron in the samples were determined photometrically following Viollier et al. (2000): 0.75 mL of suspension were reacted with 0.25 mL 2 N HCl for 1 h in a 2 mL centrifugation tube, upon which the solid phase was pelletized by centrifugation and ferrous iron was measured in the supernatant. In order to determine the dissolved ferrous iron concentration, 1 mL of the sample was filtered through a 0.2 μm poresize Acrodisc GHP filter into 2 N HCl solution. Acidification prevented oxidation of Fe(II). Extracts and filtered samples were

diluted with demineralized water to bring the final ferrous iron concentrations below 66 μmol L^{-1} prior to measurement.

2.4.4. Thermomagnetic analysis

Thermomagnetic analyses were performed with a modified horizontal Curie balance at the Paleomagnetism Laboratory, Utrecht University (Mullender et al., 1993). The field strength was varied between 150 mT and 300 mT, or between 225 mT and 300 mT for samples with high magnetite contents. Samples underwent a sequence of four heating and cooling cycles: 20–250–180 °C, 180–420–350 °C, 350–600–500 °C and 500–720–20 °C. The temperature treatment was performed in air and heating was done with a gradient of 10 °C min^{-1}.

Table 1
Equilibrium constants at 298 K for aqueous phase and surface reactions

Reaction	log β I=0 M	Ref.
$UO_2^{2+}+H_2O\leftrightarrow UO_2OH^+ + H^+$	−5.2	a
$UO_2^{2+}+2H_2O\leftrightarrow UO_2(OH)_2aq + 2H^+$	−12.0	a
$UO_2^{2+}+3H_2O\leftrightarrow UO_2(OH)_3^- + 3H^+$	−19.2	a
$UO_2^{2+}+H_2O\leftrightarrow UO_2(OH)_4^{2-} + 4H^+$	−33.0	a
$2UO_2^{2+}+H_2O\leftrightarrow (UO_2)OH^{3+} + H^+$	−2.8	a
$2UO_2^{2+}+2H_2O\leftrightarrow (UO_2)_2(OH)_2^{2+} + 2H^+$	−5.63	a
$3UO_2^{2+}+4H_2O\leftrightarrow (UO_2)_3(OH)_4^{2+} + 4H^+$	−11.9	a
$3UO_2^{2+}+5H_2O\leftrightarrow (UO_2)_3(OH)_5^{2+} + 5H^+$	−15.56	a
$3UO_2^{2+}+7H_2O\leftrightarrow (UO_2)_3(OH)_7^{2+} + 7H^+$	−31.0	a
$4UO_2^{2+}+7H_2O\leftrightarrow (UO_2)_4(OH)_7^{2+} + 7H^+$	−21.9	a
$UO_2^{2+}+CO_3^{2-}\leftrightarrow UO_2CO_3(aq)$	9.68	a
$UO_2^{2+}+2CO_3^{2-}\leftrightarrow UO_2(CO_3^{2-})_2^{2-}$	16.94	a
$UO_2^{2+}+3CO_3^{2}\leftrightarrow UO_2(CO_3^{2-})_3^{4-}$	21.6	a
$2UO_2^{2+}+CO^{32-}+3H_2O\leftrightarrow (UO_2)_2(OH)_3CO_3^- + 3H^+$	−0.86	a
$UO_2^{2+}+Lac^-\leftrightarrow UO_2Lac^+$	3.18	b
$UO_2^{2+}+2Lac^-\leftrightarrow UO_2(Lac)_2aq$	5.15	b
$UO_2^{2+}+3Lac^-\leftrightarrow UO_2(Lac)_3^-$	6.02	b
$Fe^{2+}+H_2O\leftrightarrow FeOH^+ + H^+$	−9.5	c
$Fe^{2+}+2H_2O\leftrightarrow Fe(OH)_2aq + 2H^+$	−20.6	c
$\equiv FeOH+H^+\leftrightarrow \equiv FeOH_2^+$	8.08	c
$\equiv FeOH\leftrightarrow \equiv FeO^- + H^+$	−8.82	c
$\equiv FeOH+Fe^{2+}\leftrightarrow \equiv FeOFe^+ + H^+$	−1.15	c
$\equiv FeOH+Fe^{2+}+H_2O\leftrightarrow \equiv FeOFeOH + H^+$	−10.05	c
$\equiv FeOH+UO_2^{2+}+H_2O\leftrightarrow \equiv FeOUO_2OH + 2H^+$	−4.65	c
$2UO_2^{2+}+Lac^-+H_2O\leftrightarrow 2UO_2(c)+Ace^-+HCO_3^- + 5\ H^+$	21.95	d
$2\alpha-Fe_2O_3+Lac^-+7H^+\leftrightarrow 4Fe^{2+}+Ace^-+HCO_3^- + 5H_2O$	43.39	e

[a] Grenthe et al. (1992).
[b] Constants were taken from the JESS database (May and Murray, 1991a,b, 1993).
[c] Liger et al. (1999). The constant capacitance model was used with a specific capacitance of 1.98 F m^{-2} and a site density on hematite of 2.07 sites nm^{-2}.
[d] Calculated by combining the half-reaction of lactate (Lac^-) oxidation to acetate (Ace^-) (Morel and Hering, 1993) with the equilibria for uranium reduction and uraninite solubility (Langmuir, 1997).
[e] Calculated by combining equilibrium constants for lactate oxidation, ferric iron reduction and hematite solubility taken from Morel and Hering (1993).

2.4.5. Thermodynamic equilibrium calculations

MINEQL+ 4.06 was used to calculate equilibrium solution and surface speciation in the experimental systems. Table 1 summarizes the stability constants used in the calculations.

3. Results

3.1. Abiotic reduction of U(VI)

In the abiotic reduction experiments, where ferrous iron was added to hematite suspensions as a $FeSO_4$ solution, the U(VI) concentration decreased rapidly to about 50% of its initial value within the first hour of reaction (Fig. 1). This initial drop in concentration was in agreement with that predicted by Eq. (1) for surface catalyzed U(VI) reduction. As observed by Liger et al. (1999), U(VI) reduction slowed down after the first hour. Whereas the kinetics of the initial U(VI) reduction step were independent of the amount of hematite, this was not the case for the subsequent slow disappearance of U(VI); with higher hematite concentration, less U(VI) was recovered at the end of the experiment (Fig. 1).

3.2. Reduction of U(VI) in the presence of S. putrefaciens

Dissimilatory reduction of hematite by both strains of *S. putrefaciens*, 200R and U14, produced a build-up of about 0.5 mM total ferrous iron within 48 h, at which point U(VI) was added. Uranium (VI) reduction in the bacteria+hematite incubations was similar to that observed in the abiotic experiments. Within 1 h, about 50% of the initial U(VI) was removed, followed by much slower reduction. After the first hour, the U(VI) reduction rates were similar to those

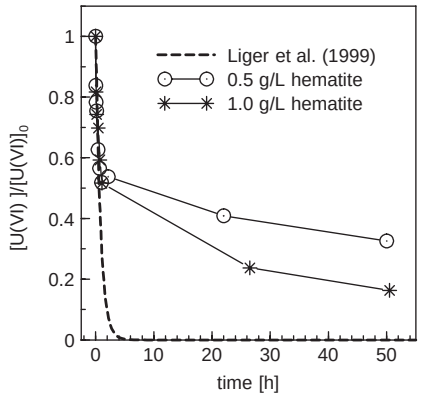

Fig. 1. Abiotic U(VI) reduction in the presence of different concentrations of nanoparticulate hematite. The broken line shows the predicted uranyl concentration in the presence of 0.5 g L^{-1} hematite calculated with the rate model of Liger et al. (1999) for the initial fast reduction step (Eq. (1) in text). ($[U(VI)]_0 = 5 \times 10^{-7}$ M, Fe(II) = 1.6×10^{-4} M, pH 7.5, 0.1 M $NaNO_3$ ionic medium, 25 °C.).

obtained in the abiotic experiments, at the same hematite concentration. Table 2 summarizes the rates of the fast and subsequent slow reduction steps under various experimental conditions.

Reduction of U(VI) in the bacteria + hematite suspensions was virtually identical for the experiments with strain 200R and strain U14 (Tables 2 and 3). However, much less U(VI) was reduced when hematite was absent. In fact, no significant decrease in U(VI) concentration was detected during the first 3 h after U(VI) was added (Table 3). After 24 h, about 27% of the initial U(VI) had been reduced by strain 200R, while more than 90% of the initial U(VI) was recovered in the incubations with strain U14 (Table 3).

Table 2
Reduction rates of U(VI) in abiotic controls, and in the presence of *S. putrefaciens* ($[U(VI)]_0 = 5 \times 10^{-7}$ M)

Bacteria strain	Hematite (g L^{-1})	$Fe(II)_{tot}$ (mM)	Time interval (h)	Average rate (M min^{-1})
No	0.53	0.16	0–1	3.4×10^{-9}
No	0.53	0.16	1–50	2.8×10^{-11}
200R	0.53	0.5	0–1	3.2×10^{-9}
200R	0.53	0.5–0.8	5–75	2.5×10^{-11}
U14	0.53	0.5	0–1	3.5×10^{-9}
U14	0.53	0.5–0.8	5–75	2.0×10^{-11}
200R	no	no	0–3	1.2×10^{-10}
200R	no	no	3–24	7.3×10^{-11}
U14	no	no	0–3	n.d.
U14	no	no	3–24	1.5×10^{-11}

Table 3
U(VI) recovery in incubations with *S. putrefaciens* as a function of time after uranyl addition ($[U(VI)]_0 = 5 \times 10^{-7}$ M)

Bacteria	Hematite	$[U(VI)]/[U(VI)]_0$			
		1 h	3 h	24 h	75 h
200R	+	0.51 ± 0.05			0.27 ± 0.05
U14	+	0.47 ± 0.05			0.26 ± 0.05
200R	−		0.96 ± 0.05	0.74 ± 0.05	
U14	−		1.05 ± 0.06	0.91 ± 0.10	

The results clearly imply that the rapid drop by about 50% of the U(VI) concentration during the first hour of reaction was caused by the presence of hematite. The ability of the organism to grow (200R) or not (U14) on U(VI) as sole electron acceptor did not seem to affect the initial rapid U(VI) reduction step, nor the subsequent slow reduction kinetics. Thus, in the hematite suspensions, the primary role of *S. putrefaciens* appeared to be the production of ferrous iron, which then reduced U(VI).

3.3. Effect of bicarbonate on iron respiration

Addition of *S. putrefaciens* to hematite suspensions initiated iron reduction without a measurable lag time (Fig. 2). Reduction rates did not vary depending on whether the bacteria were grown under aerobic or anaerobic conditions (data not shown). Increasing

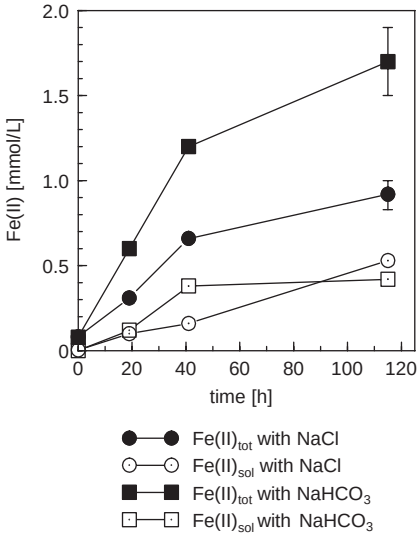

Fig. 2. Soluble and total ferrous iron production in hematite + bacteria incubations.

the hematite concentration from 0.5 to 2.0 g L^{-1} only resulted in a relatively small increase in the reduction rate, indicating that the availability of the electron acceptor was not limiting iron reduction (data not shown). However, addition of 45 mM bicarbonate to hematite + bacteria incubations approximately doubled the amount of total ferrous iron produced over the course of the experiments (Fig. 2).

Concentrations of total Fe(II) produced by iron respiration were generally more than two times higher than the concentrations of dissolved Fe(II) (Fig. 2). Hence, most Fe(II) produced during the incubation experiments was removed from solution. Sorption of Fe(II) to the bacterial cell walls was negligible under the experimental conditions (data not shown). Without bicarbonate, the distribution of Fe(II) between aqueous solution and solid phase agreed with theoretical speciation calculations based on the surface complexation model of Fe(II) to the hematite surface proposed by Liger et al. (1999) (Fig. 3). In abiotic controls addition of 45 mM bicarbonate resulted in about 10–15% higher concentrations of hematite bound Fe(II) at similar total Fe(II) concentrations (Fig. 3). In the bacteria + hematite experiments with bicarbonate, solid bound Fe(II) did not approach a constant value with increasing $Fe(II)_{tot}$ concentration, but continued to increase well beyond the sorption capacity of the hematite (Fig. 3) suggesting the formation of a Fe(II) containing precipitate.

In sharp contrast to all other experiments, during the bacteria + hematite experiments with added bicarbonate the color of the suspension changed from red to black. This change was first noticeable during the sampling performed 40 h after starting the experiments. The solids collected at the end of the experiments further exhibited the highest magnetization at room temperature (30 A m^2 kg^{-1}, Fig. 4). Without added bicarbonate, magnetization at room temperature was less than 5 A m^2 kg^{-1}. The magnetic properties of the solid phase in the abiotic controls supplemented with $FeSO_4$ did not differ from those of pure hematite, which had an initial magnetization of less than 1 A m^2 kg^{-1}.

The magnetization of the solid samples decreased when heated in air (Fig. 4). At temperatures higher than 600 °C, magnetization was less than 1 A m^2 kg^{-1} in all samples. The decrease in magnetization is caused partially by irreversible transformation of the solid phase, and partially by the reversible temperature dependence of magnetization. The contribution of the reversible temperature dependence to the decrease in magnetism was identified by cooling and heating

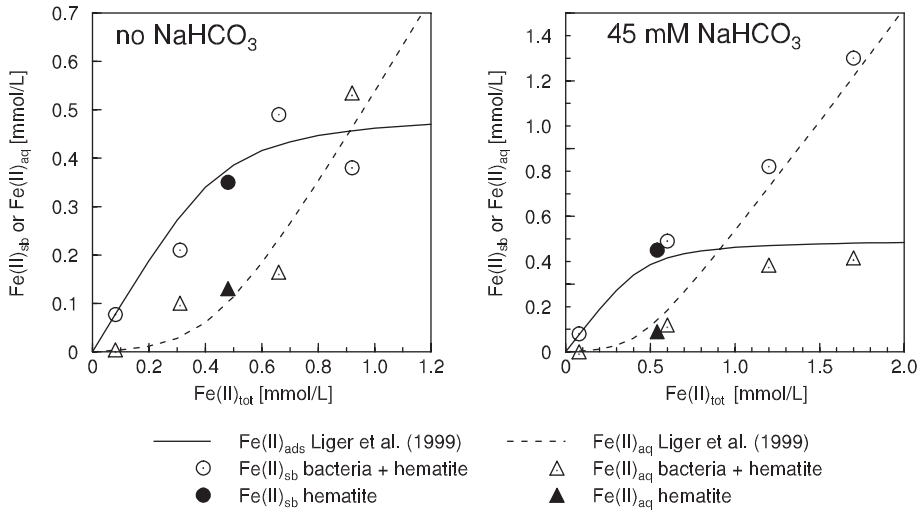

Fig. 3. Dissolved (aq) and solid-bound (sb) Fe(II) in bacteria + hematite experiments and abiotic controls. The solid and broken lines represent the predicted concentrations of adsorbed and dissolved Fe(II) calculated with the surface complexation model of Liger et al. (1999). The excess removal of Fe(II) from solution in the experiments in which $NaHCO_3$ was added is attributed to the precipitation of magnetite (see text for complete discussion).

cycles during the heating procedure. Magnetization of the samples taken from bacteria+hematite experiments with bicarbonate vanished reversibly at 580 °C, which is the Curie temperature of magnetite (Krupicka and Novak, 1982). Taken together, the observations indicate that magnetite formed in bacteria+hematite experiments with added bicarbonate.

3.4. Effect of bicarbonate on uranium adsorption and reduction

Hematite and bacteria both efficiently sorbed U(VI) in the absence of added bicarbonate (Table 4). About 10–15% of added U(VI) remained in solution, regardless of whether only bacteria, only hematite, or both were present in the experimental suspensions. However, the bicarbonate amendments affected binding of U(VI) to hematite and bacteria differently. Upon addition of 45 mM dissolved bicarbonate, U(VI) sorption to the bacteria was inhibited, while about one third of the added U(VI) remained sorbed to hematite (Table 4).

Without added bicarbonate, reduction of U(VI) in bacteria+hematite experiments was similar to that in abiotic controls (Fig. 5). After 24 h, approximately two times less U(VI) was recovered than in the experiments containing bacteria but no hematite. These observations are in agreement with those described in Section 3.2, indicating that abiotic reaction of U(VI) with Fe(II) was the dominant U(VI) reduction pathway in bacteria+hematite

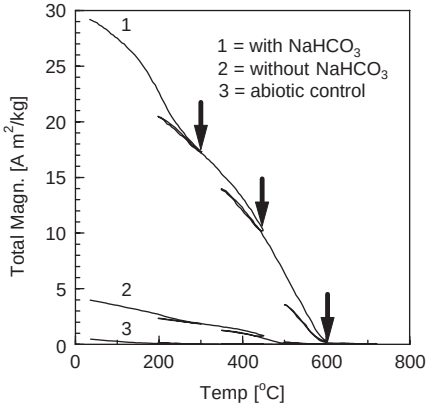

Fig. 4. Thermomagnetic properties of the solid phases recovered at the end of hematite+bacteria experiments and abiotic controls. The arrows indicate the temperatures at which a cooling–heating cycle was initiated.

Table 4
Fraction of added U(VI) remaining in solution measured in samples retrieved about 5 min after uranyl addition to experimental suspensions ($[U(VI)]_0 = 5 \times 10^{-7}$ M)

	$[U(VI)aq]/[U(VI)]_0$	
	No bicarbonate addition	45 mM bicarbonate
Bacteria only	0.16 ± 0.04	1.06 ± 0.06
Hematite only	0.10 ± 0.05	0.66 ± 0.11
Bacteria+hematite	0.11 ± 0.05	0.56 ± 0.04

experiments. That is, in the presence of hematite, *S. putrefaciens* 200R contributed to the reduction of U(VI) primarily by producing Fe(II), rather than reducing U(VI) enzymatically.

Addition of 45 mM bicarbonate slowed down U(VI) reduction in the abiotic controls, as well as in the bacteria-only experiments (Fig. 5). As expected, the formation of aqueous uranyl-carbonate complexes interfered with surface catalyzed reduction by Fe(II) and direct enzymatic reduction by *S. putrefaciens*. However, an inhibitory effect of bicarbonate in experiments with bacteria+hematite was only noticeable for the first sample, taken after 20 h of reaction, when the remaining U(VI) concentrations were similar to those in the abiotic controls, but higher than when no bicarbonate was added. After 40 h, the extent of U(VI) reduction in hematite+bacteria experiments was similar with or without added bicarbonate, while after 115 h lower U(VI) concentrations were recovered in the presence of added bicarbonate. Hence, in the presence of dissolved bicarbonate, an additional sink for U(VI), other than enzymatic reduction or hematite catalyzed reduction by Fe(II), substantially contributed to the decrease in U(VI) concentration. This sink, therefore, coincided with the inferred formation of magnetite in the bacteria+hematite experiments with added bicarbonate (Section 3.3).

4. Discussion

4.1. Competition between abiotic and enzymatic uranium reduction

A common assumption is that microbial communities, if given a choice, use the energetically most favorable terminal electron acceptor for respiration. Comparison of the energetics of lactate oxidation by

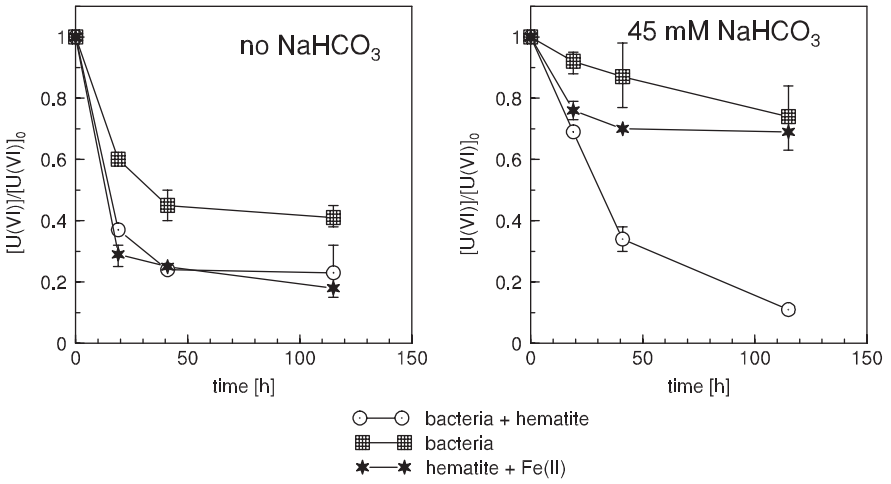

Fig. 5. Uranyl reduction without and with bicarbonate addition ($[U(VI)]_0 = 5 \times 10^{-7}$ M).

Fe(III) and U(VI) under the experimental conditions shows that the latter is the thermodynamically favored electron acceptor (Fig. 6). The free energy yield of reduction of U(VI) coupled to lactate oxidation decreases by about 40 kJ mol^{-1} in the presence of hematite, because of adsorption of U(VI) to the oxide surface. Even then, U(VI) respiration remains energetically more favorable than Fe(III) respiration. The observed reduction kinetics in bacteria+hematite experiments, however, argue against significant direct U(VI) respiration.

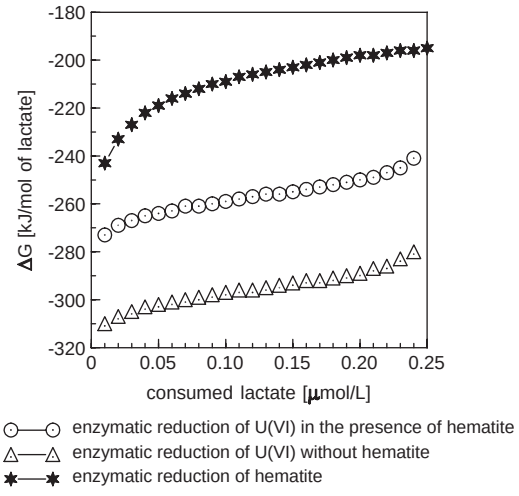

Fig. 6. Calculated free energies of reduction of U(VI) or Fe(III) coupled to the oxidation of lactate to acetate as a function of the amount of lactate consumed. Calculations were performed using the equilibrium constants in Table 1 and the conditions of the hematite+bacteria incubations without bicarbonate addition. The range of lactate consumption corresponds to the complete reduction of added U(VI) to U(IV).

Reduction of U(VI) in the bacteria+hematite experiments run without added bicarbonate is characterized by an initial fast reaction, followed by much slower kinetics. Furthermore, U(VI) reduction kinetics in these experiments is very similar to those observed in abiotic controls containing hematite, but no bacteria. Initial rates in the presence of hematite are between 3.2×10^{-9} and 3.5×10^{-9} M min^{-1}, irrespective of whether Fe(II) is produced by iron respiration or added as $FeSO_4$ solution (Table 2). Without hematite, rates of enzymatic U(VI) reduction by *S. putrefaciens* strain 200R are more than one order of magnitude lower (Table 2). Together, the results indicate that mineral surface catalyzed reduction of U(VI) by Fe(II), as proposed by Liger et al. (1999), is kinetically the more efficient reduction mechanism, at least during the fast initial reaction step.

Competition between abiotic and enzymatic reduction of U(VI) can be explained in part as a competition between the two different sorbents of U(VI) in the experiments: the hematite surfaces and the bacterial cell walls. The mineral surface catalyzed reduction requires the adsorption of U(VI) onto the hematite particles, as expressed by rate Eq. (1). Observation of uraninite particles at the surface of bacteria (Abdelouas et al., 2000; Suzuki et al., 2002) or in the periplasmic space (Liu et al., 2002) similarly implies

that U(VI) must bind to sites at the surface or inside the cell wall prior to enzymatic reduction.

The similar initial uranium reduction rates in abiotic controls and bacteria+hematite experiments suggest that hematite is a stronger sorbent of U(VI) than the bacterial cell walls. This is consistent with the observed response of U(VI) sorption to the addition of dissolved bicarbonate (Table 4). While aqueous uranyl-carbonate complexation completely removes all U(VI) bound to the bacteria, a significant part of U(VI) remains sorbed to the hematite. As a result, the relative inhibiting effect of dissolved carbonate on the initial U(VI) reduction kinetics in control experiments with bacteria, but without hematite, is larger than in the control experiments with hematite, but no bacteria (Fig. 5). Thus, we propose that efficient adsorption of U(VI) by hematite at near-neutral pH reduces the availability of U(VI) for enzymatic reduction when both bacteria and hematite are present.

Binding of U(VI) to hematite may also inhibit enzymatic reduction beyond the initial fast reduction step. Liger et al. (1999) proposed that the slowing down of surface catalyzed U(VI) reduction by Fe^{2+} may be due to the formation of mixed oxidation state uranium oxides, or the coprecipitation of U(VI) with ferric (hydr)oxides formed by oxidation of adsorbed Fe^{2+}. Trapping of uranyl ions into mixed oxidation-state precipitates would also inhibit the enzymatic reduction process, by limiting the access of the bacteria to U(VI).

4.2. Influence of bicarbonate on microbial and abiotic reduction of uranium

As predicted by Eq. (1), uranium reduction via the mineral surface catalyzed pathway should slow down when formation of aqueous uranyl-carbonate complexes decreases U(VI) sorption to hematite. However, the inhibition is not complete, as shown by the measurable decrease of U(VI) concentrations with time in the abiotic controls with added $NaHCO_3$ (Fig. 5). The surface complexation model of Liger et al. (1999) for adsorption of U(VI) onto nanoparticulate hematite predicts that virtually all added U(VI) should exist as carbonate complexes in the 0.45 mM $NaHCO_3$ solution. In contrast, the results indicate that about one third of the U(VI) remains being bound to the hematite (Table 4). The formation of ternary uranyl-carbonate complexes at the hematite surface, as proposed by Waite et al. (1994) for uranyl adsorption to ferrihydrite, could account for the discrepancy between predicted and observed adsorption of U(VI). Such ternary surface complexes are not included in the model of Liger and coworkers (Table 1). They may also explain why the added bicarbonate does not completely inhibit surface catalyzed reduction of U(VI) but only lowers the reduction rates.

The inhibiting effect of bicarbonate on U(VI) reduction in bacteria-only experiments illustrates the key role of U(VI) speciation in enzymatic reduction kinetics. In a similar vein, Haas and Dichristina (2002) found that rates of bacterial Fe(III) reduction in the presence of dissolved chelating agents correlate inversely with the thermodynamic stability constants of the Fe(III)-organic complexes. As for Fe(III), the bioavailability of U(VI) is decreased by the presence of ligands that interfere with U(VI) uptake at the cell wall. This conclusion is supported by the effect of bicarbonate addition on the initial U(VI) partitioning measured in the bacteria-only control experiments (Table 4). Without bicarbonate amendment most of the added U(VI) associates with the cells, while almost all U(VI) remains in solution upon addition of 45 mM $NaHCO_3$. The strong sorption of U(VI) onto the cell wall of *S. putrefaciens* in the absence of added bicarbonate agrees with the observations and equilibrium speciation model calculations of Haas et al. (2001) under comparable experimental conditions.

In hematite+bacteria incubations amended with bicarbonate, about 90% of the U(VI) is reduced by the end of the experiments (Fig. 5). In these experiments, a process other than direct enzymatic reduction and hematite-catalyzed reduction by Fe(II) contributes to the removal of U(VI). This additional process appears to be linked to the formation of biogenic magnetite. Strong adsorption of uranyl onto magnetite has been reported (Sagert et al., 1989) and could lead to U(VI) reduction (El Aamrani et al., 1999; Grambow et al., 1996). Recent work by Dodge et al. (2002) shows that, during coprecipitation of U(VI) with green rust II, magnetite forms and U(VI) reduces to U(IV). The reductive capabilities of magnetite, in particular biogenic magnetite, have been demonstrated for several inorganic and organic compounds including chromium (VI) (Ellis et al., 2002), technetium (VII)

(Lloyd et al., 2000), and carbon tetrachloride (McCormick et al., 2002). Direct spectroscopic evidence for abiotic reduction of U(VI) by magnetite is forthcoming (Duro, unpublished results), although in the experiments reported here we cannot exclude that some U(VI) removal is due to structural incorporation into the newly forming magnetite.

The reduction (or possibly co-precipitation) of U(VI) by biogenic magnetite implies that in the bicarbonate amended experiments abiotic immobilization mechanisms also dominate over enzymatic reduction. Lloyd et al. (2000) and McCormick et al. (2002) investigated whether iron reducing bacteria are directly involved in the reduction of technetium and carbon tetrachloride, or whether their role is primarily to produce reductants. In both cases, the authors concluded that reduction by ferrous iron was the predominant reaction pathway. Thus, increasing evidence suggests that, under iron reducing conditions, the reduction of trace metals and trace organic compounds is mostly a byproduct of the dissimilatory reduction of reactive Fe(III) solids.

4.3. Formation of biogenic magnetite

A puzzling question is why magnetite forms in the experiments in which bacteria, hematite, and dissolved bicarbonate are added together. Although biogenic magnetite formation was first reported in magnetotactic bacteria (Blakemore, 1975; Blakemore et al., 1979), Lovley et al. (1987) showed that extracellular magnetite may form as a product of dissimilatory iron reduction. Since then magnetite has been identified in a number of studies aiming at the characterization of mineral transformations during iron reduction (Benner et al., 2002; Fredrickson et al., 1998).

Fredrickson et al. (1998) investigated the effect of different buffers on the formation of biogenic iron minerals. Under comparable conditions, of pH and bicarbonate concentrations as in our experiments, they detected siderite and magnetite formation. Siderite, however, was the dominant product. The whitish precipitates, diagnostic for siderite, observed by Fredrickson and coworkers were absent in our experiments. Fredrickson et al. (1998) used amorphous hydrous ferric oxide (HFO), while we used hematite in the incubations, suggesting that the mineralogy of the starting ferric solids may influence the formation of secondary minerals.

Hematite and HFO differ with respect to their affinity for Fe(II) (Liger et al., 1999). In carbonate-free solutions, the pH-edge for Fe(II) adsorption onto hematite is approximately two pH units lower than for ferrihydrite, which presumably has similar surface properties as the HFO used by Fredrickson et al. (1998). We hypothesize that the extent of Fe(II) adsorption and the structure of the Fe(II) surface complexes play major roles in initiating magnetite precipitation. Possibly, the formation of ternary Fe(II)-carbonate complexes is a key intermediate step leading to the formation of magnetite. Further work will be needed, however, to better constrain the mechanism of extracellular bioformation of magnetite.

5. Concluding remarks

In most suboxic environments, iron is far more abundant than uranium. Under these conditions, the experimental results presented here suggest that reaction of uranyl with ferrous iron, produced by iron respiration, should outcompete direct enzymatic U(VI) reduction. The competition, however, is expected to be modulated to a large extent by solution and surface complexation reactions of U(VI) and Fe(II), as well as by the formation of secondary iron minerals. Precipitation of magnetite, in particular, enhances the immobilization of uranium in the experimental model systems. Biogenically induced precipitation of magnetite in marine sediments (Karlin et al., 1987), soils (Maher and Taylor, 1988), and lacrustine sediments (Gibbs-Eggar et al., 1999) is well established. Whether magnetite also plays an important role in the redox cycle of uranium in these natural systems is one of the questions we wish to address in our future research.

Acknowledgments

This study was financially supported by the Netherlands Organisation for Scientific Research (NWO Pioneer Programme). We thank Thomas DiChristina for providing the bacterial strains used in this research and for helpful discussions. We also thank M.J. Dek-

kers and T.A.T. Mullender from the Paleomagnetism group at Utrecht University for help in performing the thermomagnetic analyses and for assistance regarding the interpretation of the results. The insightful and constructive comments of two anonymous reviewers are gratefully acknowledged. **[LW]**

References

Abdelouas, A., Lutze, W., Gong, W., Nuttall, E.H., Strietelmeier, B.A., Travis, B.J., 2000. Biological reduction of uranium in groundwater and subsurface soil. Sci. Total Environ. 250 (1–3), 21–35.

Benner, S.G., Hansel, C.M., Wielinga, B.W., Barber, T.M., Fendorf, S., 2002. Reductive dissolution and biomineralization of iron hydroxide under dynamic flow conditions. Environ. Sci. Technol. 36 (8), 1705–1711.

Bertrand, P.A., Choppin, G.R., 1982. Separation of actinides in different oxidation states by solvent extraction. Radiochim. Acta 31, 135–137.

Blakemore, R., 1975. Magnetotactic bacteria. Science 190 (4212), 377–379.

Blakemore, R.P., Maratea, D., Wolfe, R.S., 1979. Isolation and pure culture of a freshwater magnetic spirillum in chemically defined medium. J. Bacteriol. 140 (2), 720–729.

Blakeney, M.D., Moulaei, T., DiChristina, T.J., 2000. Fe(III) reduction activity and cytochrome content of *Shewanella putrefaciens* grown on ten compounds as sole terminal electron acceptor. Microbiol. Res. 155 (2), 87–94.

Caccavo Jr., F., Blakemore, R.P., Lovley, D.R., 1992. A hydrogen-oxidizing, iron(III)-reducing microorganism from the Great Bay estuary, New Hampshire. Appl. Environ. Microbiol. 58 (10), 3211–3216.

Cochran, J.K., Carey, A.E., Sholkovitz, E.R., Surprenant, L.D., 1986. The geochemistry of uranium and thorium in coastal marine sediments and sediment pore waters. Geochim. Cosmochim. Acta 50 (5), 663–680.

DiChristina, T.J., DeLong, E.F., 1994. Isolation of anaerobic respiratory mutants of *Shewanella putrefaciens* and genetic analysis of mutants deficient in anaerobic growth on Fe^{3+}. J. Bacteriol. 176 (5), 1468–1474.

Dodge, C.J., Francis, A.J., Gillow, J.B., Halada, G.P., Eng, C., Clayton, C.R., 2002. Association of uranium with iron oxides typically formed on corroding steel surfaces. Environ. Sci. Technol. 36 (16), 3504–3511.

El Aamrani, F., Casas, I., de Pablo, J., Duro, L., Grive, M., Bruno, J., 1999. Experimental and modeling study of the interaction between uranium (VI) and magnetite. Chem. Eng. Dep., Univ. Politecnica Catalunya, Barcelona, Spain, pp. 1–30.

Ellis, A.S., Johnson, T.M., Bullen, T.D., 2002. Fate of hexavalent chromium in the environment. Science 295 (5562), 2060–2062.

Francis, A.J., Dodge, C.J., Lu, F., Halada, G.P., Clayton, C.R., 1994. XPS and XANES studies of uranium reduction by *Clostridium* sp. Environ. Sci. Technol. 28 (4), 636–639.

Fredrickson, J.K., Zachara, J.M., Kennedy, D.W., Dong, H., Onstott, T.C., Hinman, N.W., Li, S.-M., 1998. Biogenic iron mineralization accompanying the dissimilatory reduction of hydrous ferric oxide by a groundwater bacterium. Geochim. Cosmochim. Acta 62 (19/20), 3239–3257.

Fredrickson, J.K., Zachara, J.M., Kennedy, D.W., Duff, M.C., Gorby, Y.A., Li, S.-M.W., et al., 2000. Reduction of U(VI) in goethite (α-FeOOH) suspensions by a dissimilatory metal-reducing bacterium. Geochim. Cosmochim. Acta 64, 3085–3098.

Gibbs-Eggar, Z., Jude, B., Dominik, J., Loizeau, J.-L., Oldfield, F., 1999. Possible evidence for dissimilatory bacterial magnetite dominating the magnetic properties of recent lake sediments. Earth Planet. Sci. Lett. 168 (1–2), 1–6.

Grambow, B., Smailos, E., Geckeis, H., Mueller, R., Hentschel, H., 1996. Sorption and reduction of uranium(VI) on iron corrosion products under reducing saline conditions. Radiochim. Acta 74, 149–154.

Grenthe, I., Fuger, J., Konings, R.J.M., Lemire, R.J., Muller, A.B., Nguyen-Trung, C., et al., 1992. Chemical thermodynamics. Vol. 1: Chemical thermodynamics of uranium. OECE-NEA Elsevier.

Haas, J.R., Dichristina, T.J., 2002. Effects of Fe(III) chemical speciation on dissimilatory Fe(III) reduction by *Shewanella putrefaciens*. Environ. Sci. Technol. 36 (3), 373–380.

Haas, J.R., Dichristina, T.J., Wade, R., 2001. Thermodynamics of U(VI) sorption onto *Shewanella putrefaciens*. Chem. Geol. 180, 33–54.

Ho, C.H., Miller, N.H., 1986. Formation of uranium oxide sols in bicarbonate solutions. J. Colloid Interface Sci. 113 (1), 232–240.

Hobbie, J.E., Daley, R.J., Jasper, S., 1977. Use of nucleopore filters for counting bacteria by fluorescence microscopy. Appl. Environ. Microbiol. 33 (5), 1225–1228.

Karlin, R., Lyle, M., Heath, G.R., 1987. Authigenic magnetite formation in suboxic marine sediments. Nature 326 (6112), 490–493.

Kosztolanyi, K., Nguyen, T.C., Lhote, F., Vernet, M., 1996. Reduction of uranyl complexes and precipitation of uranium oxides by hydrogen sulfide gas. Magy. Kem. F. 102 (4), 180–187.

Krupicka, S., Novak, P., 1982. Oxide spinels. In: Wohlfarth, E.P. (Ed.), Ferromagnetic Materials. North-Holland, pp. 189–304.

Langmuir, D., 1978. Uranium solution–mineral equilibria at low temperatures with applications to sedimentary ore deposits. Geochim. Cosmochim. Acta 42 (6), 547–569.

Langmuir, D., 1997. Aqueous Environmental Geochemistry. Prentice-Hall Inc.

Liger, E., Charlet, L., Van Cappellen, P., 1999. Surface catalysis of uranium (VI) reduction by iron(II). Geochim. Cosmochim. Acta 63 (19/20), 2939–2955.

Liu, C., Gorby, Y.A., Zachara, J.M., Fredrickson, J.K., Brown, C.F., 2002. Reduction kinetics of Fe(III), Co(III), U(VI), Cr(VI), and Tc(VII) in cultures of dissimilatory metal-reducing bacteria. Biotechnol. Bioeng. 80, 637–649.

Lloyd, J.R., Sole, V.A., Van Praagh, C.V.G., Lovley, D.R., 2000. Direct and Fe(II)-mediated reduction of technetium by Fe(III)-reducing bacteria. Appl. Environ. Microbiol. 66 (9), 3743–3749.

Lovley, D.R., Phillips, E.J.P., 1992. Reduction of uranium by *Desulfovibrio desulfuricans*. Appl. Environ. Microbiol. 58 (3), 850–856.

Lovley, D.R., Stolz, J.F., Nord, G.L. Jr., Phillips, E.J.P., 1987. Anaerobic production of magnetite by a dissimilatory iron-reducing microorganism. Nature 330 (6145), 252–254.

Lovley, D.R., Phillips, E.J.P., Gorby, Y.A., Landa, E.R., 1991. Microbial reduction of uranium. Nature 350 (6317), 413–416.

Maher, B.A., Taylor, R.M., 1988. Formation of ultrafine-grained magnetite in soils. Nature 336 (6197), 368–370.

May, P.M., Murray, K., 1991. JESS, a joint expert speciation system: I. Raison D'etre. Talanta 38 (12), 1409–1417.

May, P.M., Murray, K., 1991. JESS, a joint expert speciation system: II. The thermodynamic database. Talanta 38 (12), 1419–1426.

May, P.M., Murray, K., 1993. JESS, a joint expert speciation system: III. Surrogate functions. Talanta 40 (6), 819–825.

McCormick, M.L., Bouwer, E.J., Adriaens, P., 2002. Carbon tetrachloride transformation in a model iron-reducing culture: relative kinetics of biotic and abiotic reactions. Environ. Sci. Technol. 36 (3), 403–410.

Mohagheghi, A., Updegraff, D.M., Goldhaber, M.B., 1985. The role of sulfate-reducing bacteria in the deposition of sedimentary uranium ores. Geomicrobiol. J. 4 (2), 153–173.

Morel, F.M.M., Hering, J.G., 1993. Principles and Applications of Aquatic Chemistry. John Wiley & Sons Inc.

Mullender, T.A.T., Van Velzen, A.J., Dekkers, M.J., 1993. Continuous drift correction and separate identification of ferrimagnetic and paramagnetic contributions in thermomagnetic runs. Geophys. J. Int. 114, 663–672.

Obuekwe, C.O., Westlake, D.W.S., Cook, F.D., 1981. Effect of nitrate on reduction of ferric iron by a bacterium isolated from crude oil. Can. J. Microbiol. 27 (7), 692–697.

Sagert, N.H., Ho, C.H., Miller, N.H., 1989. The adsorption of uranium(VI) onto a magnetite sol. J. Colloid Interface Sci. 130 (1), 283–287.

Suzuki, Y., Kelly, S.D., Kemner, K.M., Banfield, J.F., 2002. Nanometre-size products of uranium bioreduction. Nature 470, 134.

Tebo, B.M., Obraztsova, A.Y., 1998. Sulfate-reducing bacterium grows with Cr(VI), U(VI), Mn(IV), and Fe(III) as electron acceptors. FEMS Microbiol. Lett. 162 (1), 193–198.

Viollier, E., Inglett, P.W., Hunter, K., Roychoudhury, A.N., Van Cappellen, P., 2000. The ferrozine method revisited: Fe(II)/Fe(III) determination in natural waters. Appl. Geochem. 15 (6), 785–790.

Wade, R., DiChristina, T.J., 2000. Isolation of U(VI) reduction-deficient mutants of *Shewanella putrefaciens*. FEMS Microbiol. Lett. 184 (2), 143–148.

Waite, T.D., Davis, J.A., Payne, T.E., Waychunas, G.A., Xu, N., 1994. Uranium(VI) adsorption to ferrihydrite: application of a surface complexation model. Geochim. Cosmochim. Acta 58 (24), 5465–5478.

Wersin, P., Hochella Jr., M.F., Persson, P., Redden, G., Leckie, J.O., Harris, D.W., 1994. Interaction between aqueous uranium (VI) and sulfide minerals: spectroscopic evidence for sorption and reduction. Geochim. Cosmochim. Acta 58 (13), 2829–2843.

Wielinga, B., Bostick, B., Hansel, C.M., Rosenzweig, R.F., Fendorf, S., 2000. Inhibition of bacterially promoted uranium reduction: ferric (hydr)oxides as competitive electron acceptors. Environ. Sci. Technol. 34 (11), 2190–2195.